



ELSEVIER

Available online at [www.sciencedirect.com](http://www.sciencedirect.com)

SCIENCE @ DIRECT®

Physica B 357 (2005) 6–10

PHYSICA B

[www.elsevier.com/locate/physb](http://www.elsevier.com/locate/physb)

# Composition determination of semiconductor quantum wires by X-ray scattering

C.-H. Hsu<sup>a,\*</sup>, Mau-Tsu Tang<sup>a</sup>, Hsin-Yi Lee<sup>a</sup>, Chih-Mon Huang<sup>a</sup>,  
K.S. Liang<sup>a</sup>, S.D. Lin<sup>b</sup>, Z.C. Lin<sup>b</sup>, C.P. Lee<sup>b</sup>

<sup>a</sup>Research Division, National Synchrotron Radiation Research Center, 101 Hsin-Ann Road, Hsinchu Science Park, Hsinchu 30077, Taiwan, R.O.C.

<sup>b</sup>Department of Electronics Engineering, National Chiao Tung University, Hsinchu, Taiwan, R.O.C.

## Abstract

Self-assembled semiconductor nano-structures, e.g. quantum dots and wires, have recently attracted intensive interests due to their potential applications in optoelectronic industry. Strain field, compositional profile, size, and shape are the key factors determining the physical properties of these nano-structures. However, due to their mesoscopic size, it is a challenge to accurately determine those geometric and chemical parameters. In this work, we present the structural and compositional investigation of GaAs quantum wires grown on InP(001) substrates by grazing incidence X-ray scattering. In particular, we applied resonant X-ray scattering to determine the compositional distribution within the wires. With properly chosen diffraction peak and X-ray energy range, the profile of energy scan is highly sensitive to the composition of the region with selected lattice constant. As compared to other composition determination methods, which rely on the intensity ratio either between a strong and a weak diffraction or between the same Bragg diffraction collected at different energies, the profile of energy scan is not affected by the significant intensity modulation introduced by inter-wire correlation. Therefore, this method can be applied to systems of various surface morphologies and ordered structures and still provides compositional information with high accuracy and good resolution.

© 2004 Elsevier B.V. All rights reserved.

PACS: 61.10.Eq; 68.90.+g

Keywords: X-ray scattering; Quantum wires

## 1. Introduction

Nanostructures in low-dimensional semiconductor materials, such as quantum dots, wires and wells, have attracted great attentions in recent

\*Corresponding author. Fax: +886 3 578 3813.  
E-mail address: [chsu@nsrrc.org.tw](mailto:chsu@nsrrc.org.tw) (C.-H. Hsu).

years because of their connection to fundamental physics and potential applications to semiconductor electronic and optoelectronic devices. It is well known that strain fields strongly affect their physical properties. In addition, the compositional variation within these nanostructures also plays a crucial role in governing their electronic band structure. However, the determining of compositional profile within the nano-meter scale objects is a great challenge and not too many results are available. In early works, lattice parameter was often used to deduce the composition assuming the validity of the Vegard's law, which states the lattice parameter of an alloy is a molar weighted average of consisting components' lattice parameters and is commonly applied to bulk alloy systems. However, because of the strong influence of lattice mismatch occurred at the heterostructure interface and surface relaxation due to large surface-to-volume ratio, a strain-independent method is necessary in order to accurately determine the compositional distribution of nanostructures. In 1999, Kegel et al. employed grazing incidence X-ray scattering to study the strain and inter-diffusion in InAs quantum dots grown on a GaAs(001) substrate [1,2]. In that pioneering work, the authors divided quantum dots into regions of constant lateral lattice parameter, the iso-strain region. By measuring scattered X-ray intensity distribution around the surface Bragg peak corresponding to each iso-strain region, the strain and shape of the quantum dots was reconstructed. The intensity ratio between a strong, e.g. (400), and a weak, e.g. (200), diffraction associated with the same iso-strain region was used to calculate its composition. It is well known that the atomic scattering factor of an element is a smooth function of energy except at its absorption edges, where both the magnitude and the phase of atomic scattering factor exhibit drastic changes, the anomalous effect. Anomalous X-ray scattering was later applied to determine the compositional profiles of InAs/GaAs [3], Ge/Si [4] and SiGe/Si [5] quantum dot systems. The scattering intensities associated with the same iso-strain region were measured at two different energies, one below and the other one right on or above the absorption edge of one of the consisting

elements. The composition of each iso-strain region can be determined from the ratio of intensities collected at different energies. Either the weak diffraction, (200) in the InAs case, or the diffraction with large index, (800) and (620) in the Ge/Si case, was chosen to further enhance chemical sensitivity. In this article, we present an alternative method, which does not rely on the intensity ratio between two measurements performed at either different energies or different diffractions. The profile of energy spectrum associated with each iso-strain region is utilized to extract the compositional information. Under this circumstance, the complications caused by strain independent intensity modulation, such as those induced by surface correlation, can be readily eliminated and high accuracy composition determination for systems such as InGaAs can be achieved.

## 2. Experiments

The samples studied in this work were grown on InP (001) wafers by a solid-source Varian Gen II molecular beam epitaxy system equipped with an arsenic cracker cell. After native oxide desorption at 510 °C under arsenic flux, a 0.5 μm In<sub>0.53</sub>Ga<sub>0.47</sub>As buffer layer was deposited before the growth of GaAs. The lattice mismatch between the grown In<sub>0.53</sub>Ga<sub>0.47</sub>As layer and InP wafer was less than 0.2% according to the X-ray measurement. On top of the buffer layer, various amounts of GaAs were deposited. An almost flat surface morphology was observed for 2 monolayers (ML) of deposition. Upon 3 ML GaAs deposition, a periodic wire-like morphology was observed on the surface by AFM. When deposited amount exceeds 3 ML, the wire-like morphology transforms gradually into separate islands with less and less anisotropy [6]. AFM measurements reveal that the quantum wires formed with 3 ML coverage have a height about 1.2–2.0 nm and a period about 23 nm and the length of the wires can extend over microns. Lattice mismatch of bulk GaAs with respect to InP or In<sub>0.53</sub>Ga<sub>0.47</sub>As,  $(a_{\text{GaAs}} - a_{\text{sub}})/a_{\text{sub}}$ , is -3.7%, which is about the same as the case of In<sub>0.5</sub>Ga<sub>0.5</sub>As quantum dots grown on GaAs (001)

substrates but with opposite sign. However, the evolution of surface morphology is significantly different in two cases. There have been thorough studies on the strain and composition of the InGaAs quantum dots [7] and it is interesting to find the differences between the two systems.

Grazing incidence X-ray scattering measurements were conducted at two National synchrotron radiation research center X-ray beamlines, the wiggler beamline BL17B at Taiwan light source and the Taiwan beamline BL12B2 at SPring-8. The energy of X-rays used in this work is around Ga K-absorption edge, 10.367 keV. The critical angle for total external reflection at this energy range is  $\sim 0.25^\circ$  determined from the reflectivity measurement. Grazing incident angle  $\alpha_i$  of the incoming X-rays was fixed at  $0.15^\circ$ , below sample's critical angle, to enhance the sensitivity to quantum wires. A one-dimensional position sensitive detector was employed with its window aligned along surface normal to simultaneously collect X-ray photons leaving the surface at different exit angle  $\alpha_f$ . The scattering geometry was explained in details elsewhere [7].

### 3. Results and discussions

The variations of scattered X-ray intensities of the radial scans collected at substrate (220) and

$(\bar{2}20)$  surface reflections are depicted by filled circles and solid line, respectively, in Fig. 1. A pronounced bump appears on both sides of the (220) reflection, similar to what was observed in grazing incidence small angle X-ray scattering (GISAXS) pattern when the incident X-rays impinge the sample surface along the  $[\bar{2}20]$  direction. In contrast, X-ray intensity drops monotonically away from the  $(\bar{2}20)$  reflection and no such bumps were observed, just like the GISAXS pattern with X-ray coming along the [220] direction. The presence of bumps are attributed to the periodic arrangement of the quantum wires with their axes aligned with the  $[\bar{2}20]$  direction. The peak position,  $0.0273 \text{ \AA}^{-1}$  gives an average inter-wire spacing 23 nm, in agreement with the AFM observation. It is noteworthy that the bump on the high  $q$  side of the (220) scan is more intense than the one on the low  $q$  side. Similar asymmetry was also observed on the profile of the [220] direction scans at any of the Bragg reflections with non-zero projection on the [220] direction. However, no clear sign of asymmetry was observed on either the [220] scan at the  $(\bar{2}20)$  reflection or the  $[\bar{2}20]$  scans at any surface reflection. Furthermore, no asymmetry was found in GISAXS patterns with incoming X-ray parallel to either the [220] or the  $[\bar{2}20]$  direction. Because GISAXS measurements can only probe surface morphology and is insensitive to strain, we ascribe the asymmetry in intensity distribution to the strain field within the wires. The fact that the intensity asymmetric distribution only occurs along the [220] direction, the direction across the wire axis, at those reflections with non-zero projection on the [220] direction indicates that lattice relaxation is mainly confined to the direction perpendicular to the wire axis. Since the lattice parameter of relaxed GaAs is smaller than that of the substrate, it is expected that the GaAs wires suffer a tensile stress and the scattered X-rays will concentrate at the high  $q$  side of substrate Bragg peaks. The signals at the low  $q$  side of Bragg peaks are attributed to the substrate compressively strained by the overgrown wires. On the other hand, the wire lattice along the axis is almost fully strained by the substrate lattice.

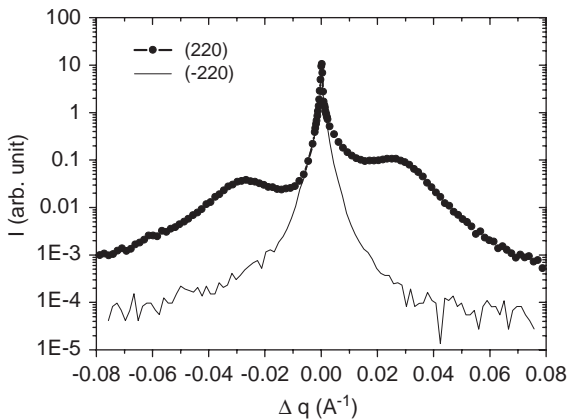


Fig. 1. The radial scan across InP (220) (filled circles) and  $(\bar{2}20)$  (solid line) surface Bragg peaks.

To obtain the chemical distribution within the wires, we take advantage of the anomalous effect. Scattering intensity is proportional to the square of a linear combination of atomic scattering factor. When the atomic scattering factor of one consisting element undergoes a drastic change as the photon energy is scanned through its absorption edge, the spectrum will exhibit a profile change accordingly. The experimental approach of this method is similar to the diffraction anomalous fine structure, DAFS, but the goal is different [8]. With a proper choice of diffraction, such as the weak diffraction of materials with the zinc-blende structure, this composition dependent profile change can be significantly enhanced and thus greatly increases the chemical sensitivity. Moreover, the pronounced bumps originated from the inter-wire spatial correlation are a function of scattering vector  $q$  but independent of photon energy. The presence of these intensity modulations only results in multiplying the strain induced intensity variation by a constant factor for each  $q$  [9]. Therefore, no special care has to be taken to eliminate the contribution from spatial correlation. Fig. 2 illustrates the scattering intensity variation of the [220] scan across the substrate (200) surface Bragg peak with  $\Delta q$  denoting the deviation in  $q$  from the substrate reflection. The diminishing in intensity to background level for  $\Delta q$

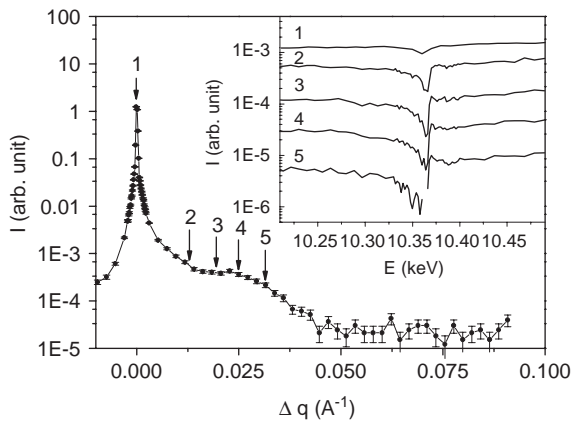


Fig. 2. The [220] scan across the substrate (200) surface reflection. The inset illustrates the energy spectra collected at various  $\Delta q$  away from the substrate (200) Bragg peak, with their positions marked by the arrows of corresponding number.

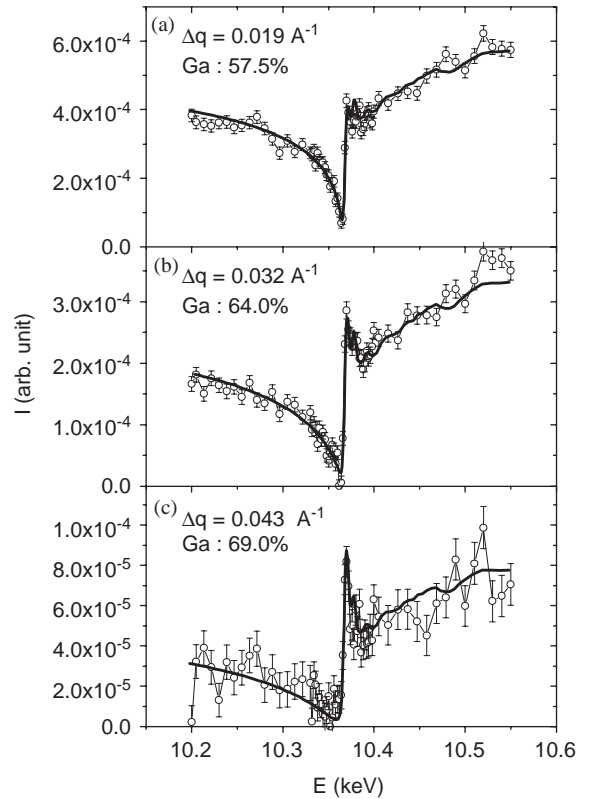


Fig. 3. The experimental spectra collected near substrate (200) reflection with  $\Delta q$  fixed at (a) 0.019, (b) 0.032, and (c) 0.043  $\text{\AA}^{-1}$  are depicted by the open circles. The solid curves are the calculated spectra with the best-fit Ga concentrations as shown by the notations.

exceeding 0.042  $\text{\AA}^{-1}$  indicates the negligible regions with lattice mismatch larger than 2%, i.e. regions with close to relaxed GaAs lattice. The inset in Fig. 2 display a series of energy spectra collected at various  $\Delta q$ 's as marked by the arrows in the [220] scan. As  $\Delta q$  increases, the profiles of the spectra exhibits obvious change; the dip progressively becomes broader and the minimum gradually moves toward lower energy. Fig. 3 displays three representative energy scans (open circles) collected near substrate (200) with  $\Delta q$  fixed at (a) 0.019, (b) 0.032, and (c) 0.043  $\text{\AA}^{-1}$ , respectively. The simulated spectra, the solid curves in Fig. 3, are calculated from the structure factor,  $F_{\text{Ga}_x\text{In}_{(1-x)}\text{As}}^{(200)} = xf_{\text{Ga}} + (1-x)f_{\text{In}} - f_{\text{As}}$ , where  $f$  stands for the

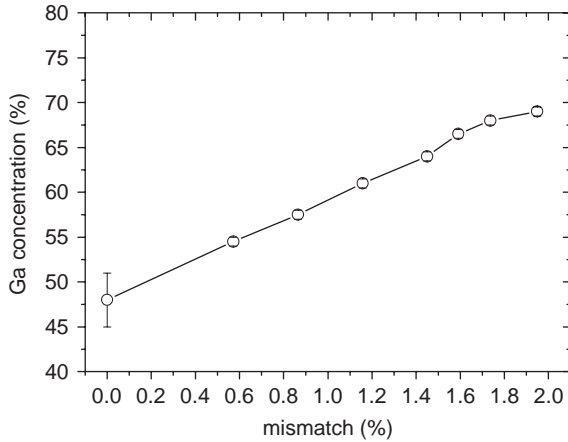


Fig. 4. The measured (open circles) Ga concentrations as a function of lattice mismatch with InP.

atomic scattering factors and  $x$  denotes the Ga concentration, with the energy dependence dispersion correction incorporated. An absorption correction is also included [8]. The details of the theoretic modeling will be published in a separate article. As shown in Fig. 3, the calculated spectra, with the best-fit Ga concentration  $x$  marked on the side, reproduce the experimental results nicely. The obtained Ga concentration  $x$  vs. lattice mismatch with respect to InP is plotted in Fig. 4. The results show that Ga concentration increases monotonically from  $\sim 48\%$  at the substrate matched lattice to  $69\%$  at  $2.0\%$  lattice mismatch. This indicates the system minimizes the strain energy via Ga–In inter-diffusion. Due to the small width of the quantum wires, there can be considerable intensity overlapping between iso-strain regions with close lattice constants, as discussed in details by Kegel et al. [2]. The resolution in lattice mismatch is estimated to be of the order of  $0.5\%$  simply based on the wire size and this can be improved by conducting the measurements at reflections of higher indices.

#### 4. Conclusion

We incorporate the anomalous X-ray effect into the iso-strain scattering method. The profile of energy scan at fixed  $q$  is a sensitive probe to the composition of the corresponding iso-strain region. We have demonstrated that the advantage of this method while being applied to the regularly arranged GaAs quantum wires, a system with strong surface correlation. No special efforts have to be put to eliminate the influence of the correlation interference peaks and the composition-strain dependence with high accuracy can be obtained.

#### Acknowledgements

The work at NSRRC was partially supported by the National Science Council of Republic of China under Contract No. NSC 92-2112-M-213-010.

#### References

- [1] I. Kegel, T.H. Metzger, P. Fratzl, J. Peisl, A. Lorke, J.M. Garcia, P.M. Petroff, *Europhys. Lett.* 45 (1999) 222.
- [2] I. Kegel, T.H. Metzger, A. Lorke, J. Peisl, J. Stangl, G. Bauer, J.M. Garcia, P.M. Petroff, *Phys. Rev. Lett.* 85 (2000) 1694.
- [3] T.U. Schulli, M. Sztucki, V. Chamard, T.H. Metzger, D. Schuh, *Appl. Phys. Lett.* 81 (2002) 448.
- [4] R. Magalhaes-Paniago, G. Medeiros-Ribeiro, A. Malachias, S. Kycia, T.I. Kamins, R. Stan Williams, *Phys. Rev. B* 66 (2002) 245312.
- [5] T.U. Schulli, J. Stangl, Z. Zhong, R.T. Lechner, M. Sztucki, T.H. Metzger, G. Bauer, *Phys. Rev. Lett.* 90 (2003) 66105.
- [6] S.D. Lin, C.P. Lee, W.H. Hsieh, Y.W. Suen, *Appl. Phys. Lett.* 81 (2002) 3007.
- [7] C.-H. Hsu, H.-Y. Lee, Y.-W. Hsieh, Y.P. Stetsko, N.T. Yeh, J.-I. Chyi, D.Y. Noh, M.-T. Tang, K.S. Liang, *Physica B* 336 (2003) 98.
- [8] H. Stragier, J.O. Cross, H.J. Rehr, L.B. Sorensen, *Phys. Rev. Lett.* 69 (1992) 3064.
- [9] I. Kegel, T.H. Metzger, J. Peisl, P. Schittenhelm, G. Abstreiter, *Appl. Phys. Lett.* 74 (1999) 2978.